Biomedical Microdevices (2018) 20:82
https://doi.org/10.1007/s10544-018-0329-x

Bionic 3D spheroids biosensor chips for high-throughput and dynamic drug screening

Qian Wu[1,2] · Xinwei Wei[1] · Yuxiang Pan[1] · Yingchang Zou[1] · Ning Hu[1,2] · Ping Wang[1,2]

Abstract

To perform the drug screening, planar cultured cell models are commonly applied to test efficacy and toxicity of drugs. However, planar cultured cells are different from the human 3D organs or tissues *in vivo*. To simulate the human 3D organs or tissues, 3D spheroids are developed by culturing a small aggregate of cells which reside around the extracellular matrix and interact with other cells in liquid media. Here we apply lung carcinoma cell lines to engineer the 3D lung cancer spheroid-based biosensor using the interdigitated electrodes for drug efficacy evaluation. The results show 3D spheroid had higher drug resistance than the planar cell model. The anticarcinogen inhibition on different 3D lung cancer spheroid models (A549, H1299, H460) can be quantitatively evaluated by electric impedance sensing. Besides, we delivered combination of anticarcinogens treatments to A549 spheroids which is commonly used in clinic treatment, and found the synergistic effect of cisplatin plus etoposide had higher drug response. To simultaneously test the drug efficacy and side effects on multi-organ model with circulatory system, a connected multiwell interdigitated electrode arraywas applied to culture different organoid spheroids. Overall, the organization of 3D cancer spheroids-based biosensor, which has higher predictive value for drug discovery and personalized medicine screening, is expected to be well applied in the area of pharmacy and clinical medicine.

Keywords Bionic 3D spheroid chips · 3D cancer spheroid · Cancer model · Drug screening · Personalized medicine

1 Introduction

The conventional process of drug screening is lengthy and extremely expensive through planar cultured cell model (Nam et al. 2015). Such two-dimensional (2D) *in vitro* assays are difficult to imitate the *in vivo* complexity of 3D tissues, and it shows low predictive ability for clinical trial of drug test (Hay et al. 2014). Meanwhile, an increasing number of 3D cell culture researches are performed due to cells in 3D environment behave differently from those in 2D culture, and higher predictive value was reported for drug discovery and screening (von der Mark et al. 1977; Li et al. 2010; Bierwolf et al. 2011).

In the 3D cell culture model, most common approach is to encapsulate cells in the hydrogel (Tibbitt and Anseth 2009). As the cells suspend in the hydrogel, unequal chemical concentrations are received from surrounding environment (Lei et al. 2018). Culture of 3D spheroid is a small aggregate of cells grows free of foreign materials (scaffold-free technique) (Fennema et al. 2013). Cells in whole organotypic *in vitro* 3D spheroid reside around the extracellular matrix and they can interact with cells from their original microenvironment, so 3D spheroid is an excellent model for probing cell-cell and cell-matrix interactions (Lin and Chang 2008). 3D spheroids with cells which were surrounded by extracellular matrix as in the human body represent a promising therapy prediction model for personalized medicine screening (Veelken et al. 2017). Moreover, the approach of spheroid culture can adapt to high-throughput screening instruments by hanging drop method (Tung et al. 2011). Therefore, spheroid culture is a biomimetic and high-throughput approach to investigate

Electronic supplementary material The online version of this article (https://doi.org/10.1007/s10544-018-0329-x) contains supplementary material, which is available to authorized users.

✉ Ning Hu
huning@zju.edu.cn

✉ Ping Wang
cnpwang@zju.edu.cn

[1] Biosensor National Special Laboratory, Key Laboratory of Biomedical Engineering of Ministry of Education, Department of Biomedical Engineering, Zhejiang University, Hangzhou 310027, China

[2] State Key Laboratory of Transducer Technology, Chinese Academy of Sciences, Shanghai 200050, China

Published online: 15 September 2018

pharmacological efficacy and intercellular interactions in many field of medicine or basic science (Fennema et al. 2013; Gao et al. 2017). Additionally, compared to 3D spheroid formed by normal cells, spheroids formed by carcinoma cell line can mimic tumor *in vivo* that lacks oxygen and nutrition in the center due to the rapid proliferation. Moreover, it can reflect tumor development and the therapy responses to possible anticarcinogen resistance mechanisms (Fennema et al. 2013; Árnadóttir et al. 2018; Jenkins et al. 2018).

Conventionally, drug efficacy evaluation for 3D cells was performed by staining technique such as MTT (3-(4,5-dimethylthiazol-2-yl)-2,5-diphenyltetrazolium bromide), WST-1 (water soluble tetrazolium salts-1) or CCK-8 (cell counting kit-8) assay. These trials only presented the static results of live/dead cells, but cannot monitor the cells in real time during the long-term recording. Moreover, once the cells were stained, it was impossible to be used in the following treatment. While cell electrical impedance reflected the characteristics, such as cell number, cell attachment, and cell morphology on electrodes in continuous and dynamic way (Giaever and Keese 1986; Keese et al. 2002), which had a wide range of applications, such as drug efficacy and toxicity assessment (Asphahani and Zhang 2007; Arias et al. 2010). While most of impedance biosensor studies focus on 2D cell culture. Additionally, Luongo et al. (2013) used electrical impedance to trap spheroids, and Bürgel et al. (2016) monitored spheroids suspended in medium by impedance spectroscopy, but that need complex operation and last long time period (4 days). To our knowledge, although some reports investigated anti-cancer drugs against cancer spheroids, but few reports focus on spheroid viability by electrical cell-substrate impedance sensing until now.

In this wok, we reported a system of 3D spheroids-based biosensor chips integrated with electrical impedance sensor which can be sound applied to drug discovery and screening. Besides, to mimic the drug metabolism function of different organ models, an improved multi-wells linked system which could simultaneously monitor different kinds of spheroids in the same culture environment was developed. All the details will be discussed in the following sections.

2 Material and methods

2.1 Cell lines and reagents

Three human lung carcinoma cell lines (A549, H1299 and H460) were used in this research to establish the spheroid cancer model. Cisplatin, etoposide and pemetrexed (ApexBio) were used to treat 3D spheroids. Cardiomyocyte HL-1 and hepatoblastoma HepG2 were used to establish heart and liver spheroid respectively, which could test the side effects of anticarcinogen on other organs model. Cell viability was verified by Calcein-AM/PI Double Stain Kit (Yeasen) under fluorescence microscope, and live cells would be dyed green by Calcein and dead cells would be dyed red by PI.

2.2 Fabrication of spheroid cancer model

The 2D cell lines was cultured in the standard medium containing RPMI-1640 medium (Gibco), 10% fetal bovine serum (Gibco), 100 U/ml penicillin, 100 mg/ml streptomycin (Sigma Aldrich) and 2 mM Glutamax (Gibco) at 37 °C and 5% CO_2 according to the conventional method. Cells from 2D culture in exponential growth phase were detached by 0.25% trypsin-EDTA (Gibco) and then be used to form the cell suspensions with density of 5×10^6 cells/ml (Fig. 1a). To improve the aggregation of the cells, 15 μg/ml collagen Type I from rat tail (BD Biosciences) and 2 mg/ml methylcellulose (Sigma Aldrich) were added. Then, diluent suspension was split into 35 μL droplets which containing 5000 cells by pipette, and then seeded on the inner surface of the cell culture dish's lid which made by polystyrene. Subsequently cover the lid on the dish made the droplets hanging on the top for culturing (Fig. 1a). The dish was kept in the incubator for 24 h and 5 ml PBS was added in the bottom to avoid droplet evaporation. After 24 h, every hanging droplet in the culture dish would form a spheroid, which can be collected in the centrifuge tube by pipette for further experiment. As reported, co-culture spheroids consisted of fibroblasts and endothelial cells could promote the formation of microvascular network, and also could support and modulate the migration and viability of endothelial (Metzger et al. 2011). While in this study, we need compare the drug effects between 2D and 3D culture, so the same cell line was used to reduce variable factor.

2.3 Impedance sensor and recording system

The 3D spheroid-based impedimetric system was included signal generator module which created a sinusoidal voltage with amplitude of 30 mV and frequency of 10 kHz to the interdigitated gold electrodes, and signal amplifier and filter module which converted the current signals to voltage signals. Then the signals can be recorded by the data acquisition module. Finally, the digital signals were transferred to computer to calculate the impedance value by the signal processing software. The xCELLigence real-time cell analysis (RTCA) instrument for impedance measurement was bought from ACEA Biosciences Inc., China. The software for the treatment of obtained electrochemical data was RTCA 2.1. In same physiological environment, when spheroids attached to the electrodes surface, the electric current is impeded, leading the impedance increases. As spheroids fully adhered on the electrodes and the impedance value increases slowly. For the same spheroid quantity in the well, changes in spheroid status (viability or morphology) that alter the spheroid-electrode contact will be also reflected by changes of impedance

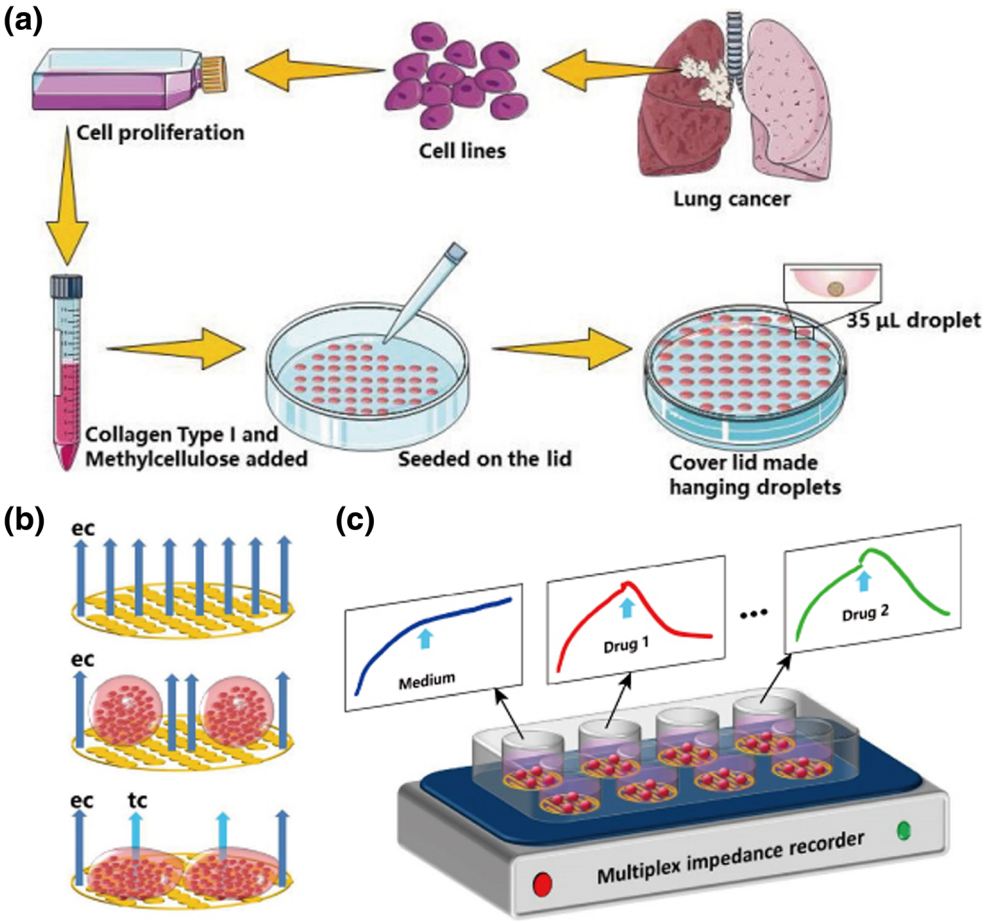

Fig. 1 **a**. The processes from tumor-derived cells to spheroid formation. Maintained tumor-derived cells in 2D liquid culture to exponential growth phase was used to form cell suspension, then pipetted in 35 μL droplets onto culture cell dish and turned upside-down resulting in hanging drops. **b**. Schematic diagram of impedance measurement principle. Frequency of 10 kHz can acquire both extracellular current (ec) and transcellular current (tc). As spheroids attached to electrodes led to increase of impedance value. **c**. Schematic overview of 3D spheroids based biosensor chips integrated with electrical impedance sensor. The spheroid culture in chip and the CI (cell index) value collect by recording system. Changes in spheroid status from different drugs that alter the cell-electrode contact will be reflected by changes in CI curves

(Fig. 1b). The value of impedance is usually normalized by cell index (CI) value for comparison. CI is the ratio of the cell impedance change ΔZ to background impedance Z_0,

$$CI = \frac{Z_{spheroid}}{Z_0} - 1$$

which excludes the impacts of electrode–electrolyte combination and parasitic elements (Zou et al. 2015; Hu et al. 2017). Therefore, the CI value can reflect the spheroid behavior like morphology, dissociation and adhesion to the electrodes. Before detection, the electrodes of every single well in sensor chip were coated with 8 μg/ml Laminin (Sigma) overnight in 4 °C refrigerator to ensure every spheroid attach to the electrodes smoothly.

2.4 Real-time monitoring of spheroid

Before the spheroid monitoring, 100 μL of PBS was used to wash the electrodes firstly and 100 μL standard medium was added to each well (diameter 5 mm) to measure the baseline of impedance Z_0. Then, 100 μL of standard medium with spheroids were added carefully to ensure all spheroids distribute symmetrically and dispersedly on the electrodes. After spheroids seeded, the sensor chip was placed in the incubator until drug treatment. Then the medium of treated groups was removed and replaced by 200 μL fresh medium with anticarcinogen. While medium of control group was removed and replaced by 200 μL fresh medium without any drug. Finally, the sensor chip was placed back to the incubator.

2.5 Multi-wells microfluidics detection

Multi-wells were linked through silicone tube which glued to the edges for avoiding leakage. The culture medium was cycled by a peristaltic pump with the speed of 300 μL/min. After ultraviolet sterilization, all the instruments, include impedance system, multi-organs-on-a-chip and peristaltic pump, were kept in the incubator. Cardiomyocyte HL-1 and hepatoblastoma HepG2 were used for the formation of heart and liver spheroid model, and the process was same as described earlier. Cisplatin (10 μM) was used as drug stimulation, and the liquid volume in silicone tube should be counted when calculate the final concentration of drug.

2.6 Data analysis

To quantify the CI response under various cells or spheroids, ΔCI values were obtained by normalizing the CI values of at certain point as 1, and regulated other CI values based on the

normalized point. Impedance response intensity was defined as CI_R which calculated by subtracting ΔCI value of the control group from the ΔCI value at the same time point of drug treated groups ($CI_R = \Delta CI_{control} - \Delta CI_{drug}$). All results were presented as mean and standard deviation from at least three independent experiments.

3 Results

3.1 Formation of spheroid

As the lung cancer is the leading cause of cancer-related morbidity and mortality globally, three kinds of lung carcinoma cells (A549, H1299 and H460) detached from 2D monolayer culture which in the exponential growth phase were assembled to form A549, H1299 and H460 spheroids as the lung cancer disease model. After suspension culture in hanging droplet for 24 h, cells were aggregated completely and formed a spheroid with about 300 μm diameter. Figure 2a showed three kinds of spheroids under bright field and fluorescent microscope. Fluorescent images merged Calcein-AM and Propidium iodide (PI) for live/dead staining, and the cell viability was all higher than 90% (Fig. 2b). Cell aggregation is the key step for spheroid formation. Once cells suspension without collagen Type I and methylcellulose, cell masses were retained a lower ability of combination and dispersed in the medium (Fig. 2c). Spheroid could survival healthily more than 5 days when fresh medium are replaced everyday (Fig. S1). During this period, cells would assemble more closely made the surface smoothly, and cell division rarely occurred in spheroid. Overall, our spheroids could be a suitable cancer model for the following trial and long-term drug test.

3.2 Dynamically monitoring of spheroids state

To validate the feasibility of spheroids detection by impedance sensor, A549, H1299 and H460 spheroids with fresh medium were pipetted to different chip wells, respectively. For the number of spheroid, we found 20 spheroids in a well were too sparse to detect (Fig. 3a), and 30 spheroids per well was the appropriate concentrations (Fig. 3b). While 40 spheroids made overlapping and different to distribute evenly (Fig. 3c). The control well only added standard medium. As long as the spheroids located on the electrodes at the bottom of chip (Fig. 3d, e), the value of impedance would increase, the maximal value

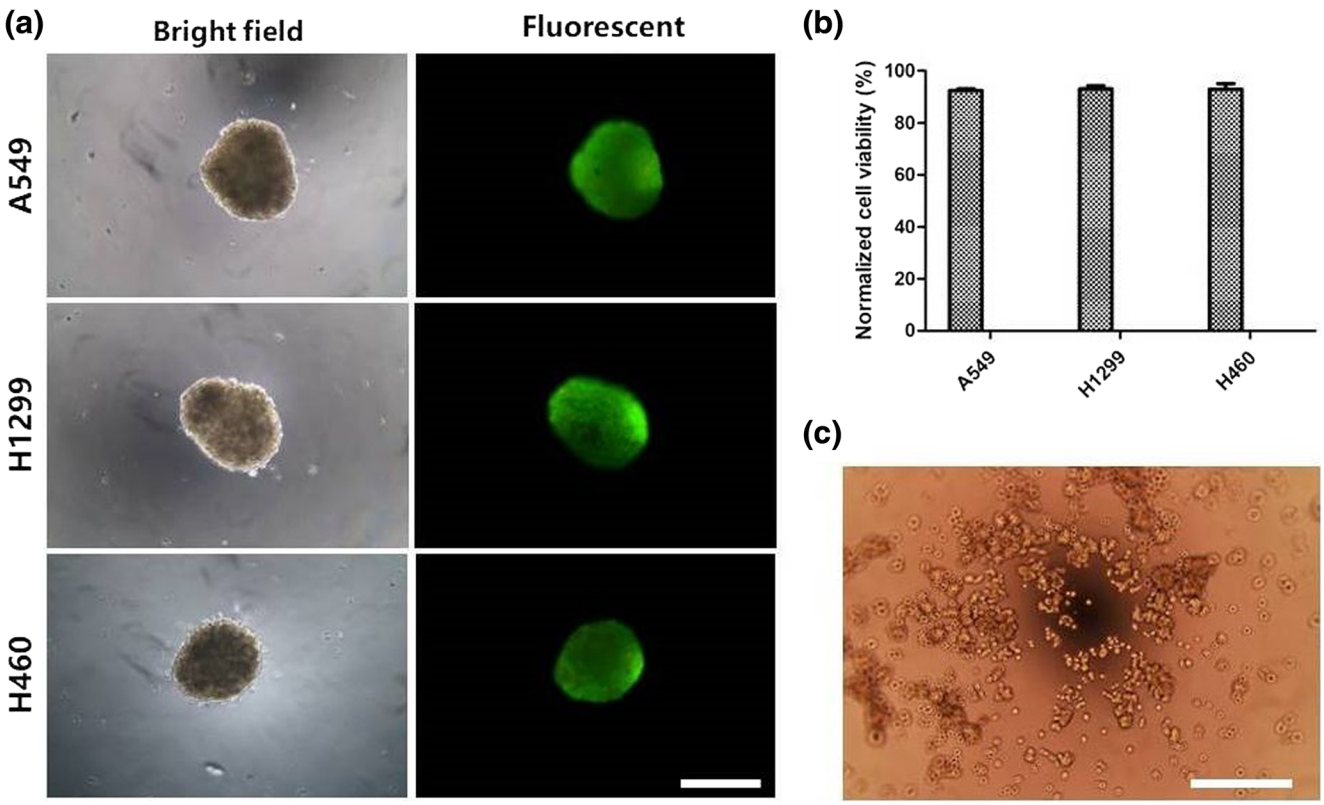

Fig. 2 **a**. The images of three kinds of spheroid under bright field and fluorescent taken by inverted microscope (scale bar 300 μm). Spheroids were formed integrated after 24 h culturing in hanging droplet and the merged live/dead staining images present high viability. **b**. The normalized cell viabilities of three kinds of spheroid were all higher than 90%. **c**. Discrete cells cluster after 24 h suspension culture by standard medium without collagen Type I and methylcellulose (scale bar 300 μm). Cell masses were retained a lower ability of combination and dispersed in the medium

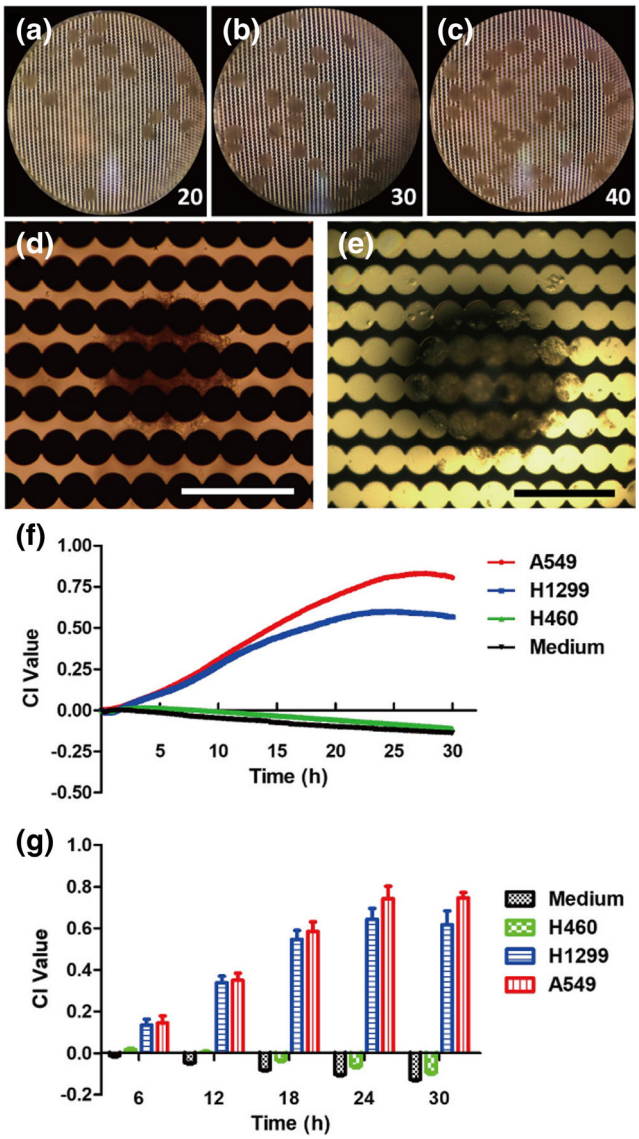

Fig. 3 **a**, **b**, **c**. The photos of 20, 30, 40 spheroids seeded in a sensor chip well, respectively, taken by stereoscopic microscope. Best concentration was 30 spheroids per well. **d**, **e**. The front and back views of spheroid attached on the interdigitated electrodes (scale bar 300 μm). **f**. The real-time impedance curves of A549, H1299 and H460 spheroid and medium control in 30 h. A549 and H1299 spheroids had favorable ability of attachment to the electrodes. **g**. Normalized CI value in specific time point, data were represented as mean ± SD from at least three independent experiments

occurred when all spheroids adhered consummately. While spheroids started necrosis and detached from the electrodes, the value decrease. In Fig. 3f, the curves of A549 and H1299 spheroids were increase over time, while H460 was a plane curve. This demonstrated that A549 and H1299 spheroids had favorable ability of attachment. However, H460 spheroids cannot adhere to the electrodes. A549 was an epithelial cell, H1299 was established from a lymph node metastasis, and this two were both non-small cell lung carcinomas, while H460 was one kind of large cell lung cancer derived from pleural effusion (ATCC: The Global Bioresource Center, https://www.atcc.org/). Cells in pleural effusion were suspended, which maybe lead H460 had less ability of attachment to the electrodes than epithelial cells. Therefore, as the lung cancer disease model, A549 and H1299 spheroids were used to test drug reaction in the following experiment. In addition, the curve of H460 and medium control was deceased slightly as time proceeded. This was because a small quantity of medium was evaporated in the incubator during long-term culturing. In order to compare with 2D cell culture, we tested different cell numbers to find which cell concentration would generate similar CI value. As shown in Fig. S2, cells were seeded at different densities ranging from 1250 to 20,000 per well, and the CI values were proportional to cell numbers. According to the linear fitting result, CI value of 8000 cells/well would similar to 30 spheroids in a well. Hence, this concentration was chosen as the 2D cell culture control.

3.3 Response to cisplatin

Usually, Chemical treatment was performed before the plateau phase started. Thus, it was easy to compare the change of CI value between medicated group and control group. A549 and H1299 spheroids attached entirely at 24 h, after that CI value tend to be stable (Fig. 3f, g). Consequently, we chose 24 h as the time point for drug treatment. Cisplatin was a broad-spectrum anticarcinogen which hindered the replication and transcription of DNA through cross-linking and forming Pt-DNA compound to damage the DNA structure. It was widely used in cancer treatment and always as the first choice for patients of non-small cell lung carcinomas. In general lung cancer cell research, the concentration of IC50 was 10 μM (Shin et al. 2014), hence 10 μM was used to treat A549, H1299 spheroids, and the corresponding 2D cells, respectively. In order to test the influence of anticarcinogen to impedance measurement, the CI values of anticarcinogens with the concentration of what we used in our experiment were detected. In Fig. S3, cisplatin, etoposide and pemetrexed with the concentration of 10 μM, 10 μM and 100 μM produce very low CI value, and those influences can be ignored in our experiment.

As a result, impedance response intensities of 2D cells were both higher than spheroids which mean the drug resistance of 2D culture cells was apparently lower than spheroids. The curves of spheroids were smooth at the beginning, and then deceased as the toxicity to cells (Fig. 4a). As the cells located at spheroid surface were exposed to cisplatin earlier than inner ones and they both need time to interact with each other. Then the integral state of the spheroid reflected on the CI values. Additionally, the cellular morphology in spheroid was globose instead of flattened cells in monolayer 2D culture, and the cells aggregated together were more easily to interact with adjacent cells and extracellular matrix. Thus, spheroid could present a general effect which more similar happened *in vivo* than 2D culture.

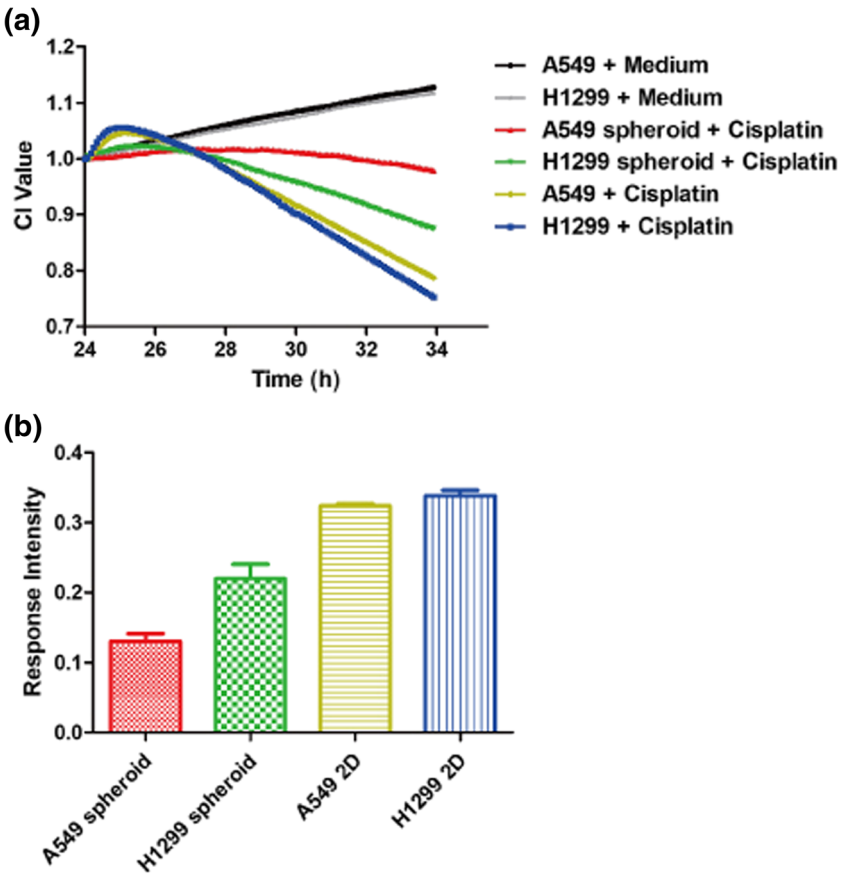

Fig. 4 **a**. A group of normalized impedance curves of different spheroids and cells responding to 10 μM cisplatin. **b**. The impedance response intensity of different spheroids and cells. Data were represented as mean ± SD from at least three independent experiments

Furthermore, as shown in Fig. 4, curves of A549 in 2D or 3D culture were both above H1299 counterparts, indicating cisplatin had a stronger inhibition to H1299. H1299 cell line has a homozygous partial deletion of the p53 protein, and lack expression of p53 protein which functions as a tumor suppressor. It can activate DNA repair proteins when DNA has sustained damage (Surget et al. 2014). Thus, the Pt-DNA compound in H1299 cells cannot be repaired by p53 pathway that leading more terrible cellular state than A549 cells. What's more, A549 cells usually express of c-Jun to protect them from apoptosis induced by cisplatin (Huang et al. 2017). Moreover, the discrepancy of impedance response intensity was more obvious in spheroid group compared with 2D cell group. The difference value for A549 spheroid and H1299 spheroid was about 0.08, while 2D culture was fairly minor (Fig. 4b). Consequently, spheroid culture was more suitable for drug screening, because it could reflect more conspicuous difference compared with 2D cell culture. In general, the system of spheroids combined with impedance sensor could not only get higher predictive results than 2D culture, but also could detect various drug effects for different kinds of cells.

3.4 Response to combination of anticarcinogens

As previous results confirmed, A549 spheroid had an efficacy of resistance to cisplatin. According to the official medical guidelines from National Comprehensive Cancer Network (NCCN: https://www.nccn.org/) for non-small-cell lung carcinoma, kinds of combined therapies were performed in clinical to reduce the drug resistance of single drug. We chose two most frequently used combined anticarcinogens therapeutic regimen, cisplatin (10 μM) plus etoposide (10 μM) and cisplatin (10 μM) plus pemetrexed (100 μM). The drug dosage was referred to the clinical practice guideline from NCCN. Considering the clinical demand to discover the best therapeutic regimen earlier, we adjusted our test schedule that delivering candidate drug in advance to 12 h. Thus the experimental period shorten from 34 h to 24 h. In this way, doctors could gain more time for early treatment.

As shown in Fig. 5a, the curve of spheroids without any drug treatment was rise gradually due to the attachment. Spheroid attachment ability reflects the general physiological state, and effective drug make spheroids cannot adhere to electrodes favorably, which leads to the decrease of CI values. According the impedance response intensity in Fig. 5b, plus etoposide performed the best efficacy. While the treatment effect of cisplatin plus pemetrexed was a little above to cisplatin. Besides, we verified the cell viability of spheroids by fluorescent conterstaining with Calcein-AM and PI. The fluorescent microscopic images shown in Fig. 5c were consistent with the results of impedance sensor detection, and spheroids

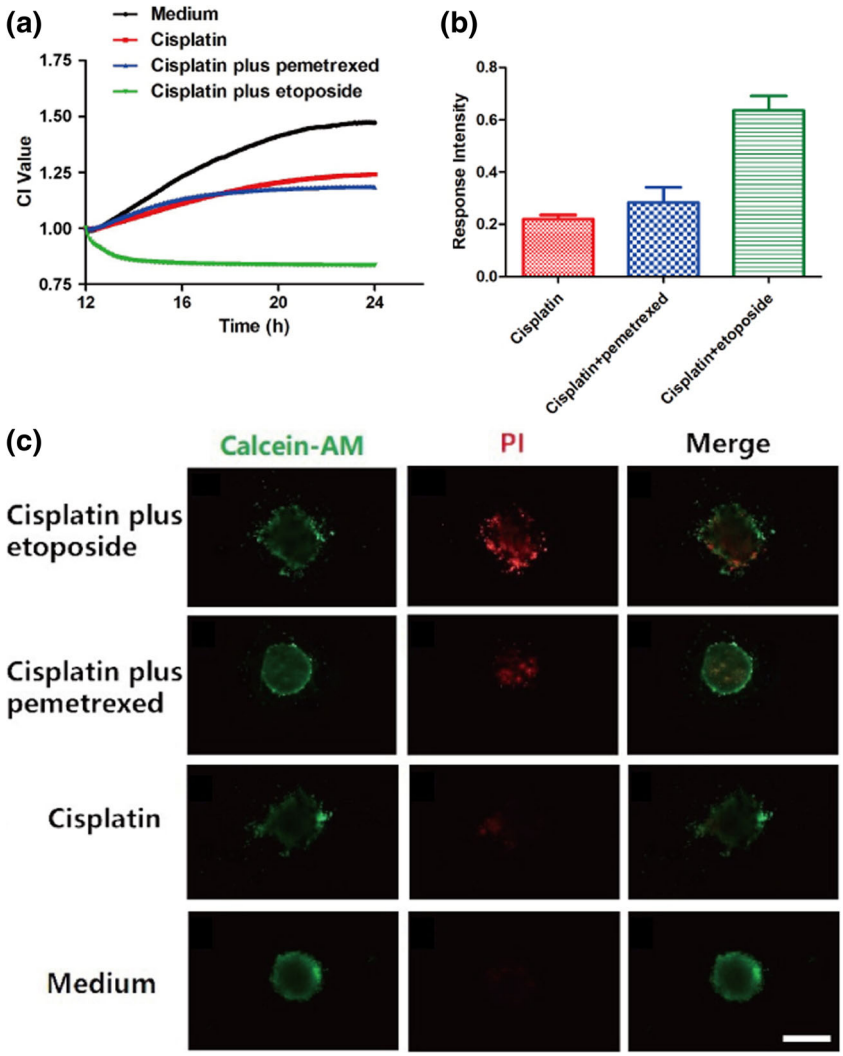

Fig. 5 **a**. A group of normalized impedance curves of A549 spheroids response to cisplatin and combined anticarcinogens therapeutic regimens from 12 h to 24 h. **b**. The impedance response intensity of A549 spheroids to different treatment. Data were represented as mean ± SD from at least three independent experiments. **c**. The microscopic images of fluorescent staining with Calcein-AM and PI for A549 spheroids which treat with cisplatin plus etoposide, cisplatin plus pemetrexed, cisplatin, and medium, respectively. Scale bar 300 μm

treat with cisplatin plus etoposide presented the major cell mortality rate.

Therefore, the spheroids-impedance sensor system can be well applied to the study of different drug efficacy aiming at a specific disease. Next, biopsy tissue samples or bronchoalveolar lavage fluid from patients with lung cancer could be test in order to find the best curative drug for subsequent treatment promptly. This patient-derived spheroid culturing method could especially contributed to personalized medicine, and make it possible for every patient to own a customized treatment plan in the future.

3.5 Simultaneous detection of multi-organs-on-a-chip by microfluidics

Drugs and their metabolites both can affect target organ or other relevant organs. It was reported that oxaliplatin (platinum derivative) and its metabolite dichloro platinum could reduce the sensitivity to therapeutic drugs though activating the nuclear factor (erythroid-derived 2)-like 2 (Nrf2) signaling pathway (Wang et al. 2014). On the other hand, ginsenoside metabolite compound K enhances the efficacy of cisplatin in lung cancer cells (Li et al. 2015). Thus, it was necessary to fabricate a chip that can simultaneously detect the physiological parameters of multi-organs. Multi-organs-on-a-chip platform integrated a single microfluidic circuitry to enable the interaction among different units, which was closer to the *in vivo* environment. We recruited A549, HL-1 and HepG2 spheroids co-culturing on the chip which represent the organs model of lung, heart and liver, respectively. Three kinds of spheroids were seeded in different wells and the flow path was cycled by peristaltic pump (Fig. 6a and Fig. S4). Cisplatin (final concentration kept in 10 μM) was added to the drug well and the fluid traversed to HL-1, A549 and HepG2 successively. This method simulated the process that anticarcinogens were injected into the vein and the blood flowed through heart at first, then come to target organ for drug function, and metabolized in liver at last. Cisplatin was added in drug well and driven by peristaltic pump which led drug delivery in order and slowly by the flow.

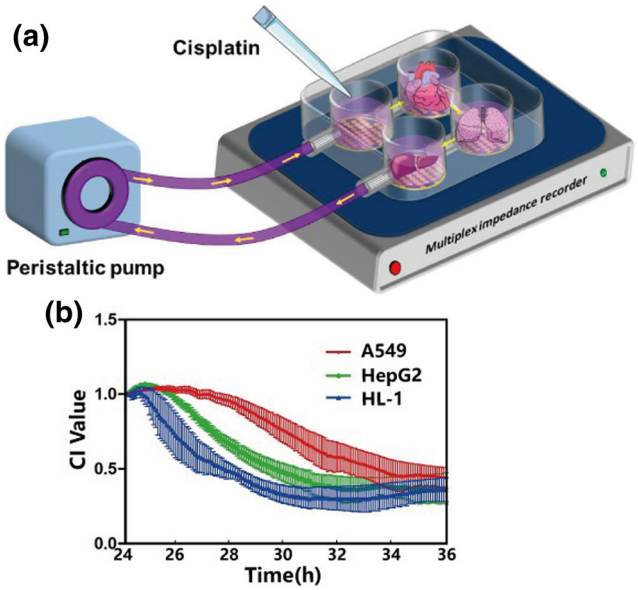

Fig. 6 **a**. The multi-organs-on-a-chip platform linked through silicone tube and cycled by peristaltic pump. Fluid with drug traversed to drug well, HL-1, A549 and HepG2 successively. **b**. Normalized cell impedance curves of different spheroid response to 10 μM cisplatin

As shown in Fig. 6b, the largest fall of CI value came from HL-1 and following by HepG2. These two kinds of spheroid were both drug sensitive, while A549 spheroid performed the strongest drug resistance. The decrease curve of HL-1 spheroid revealed that cisplatin would damage the heart, also, HepG2 spheroids were sensitive to cisplatin like previous reported (Salimi et al. 2017). Different from the results shown in Fig. 4a, the CI value curve of A549 spheroid in multi-organs-chip started to accelerate decline after 4 h drug treatment. This may be the metabolite of cisplatin from HL-1 and HepG2 spheroid which would inhibit the activity of A549 spheroid.

Hence, multi-organs-on-a-chip by microfluidics could mimic different human organs' function and their interactions, and it can be a favorable application on the research of drug effects which especially focus on the side effect to other relevant organs.

4 Conclusion

In conclusion, we reported a system of 3D spheroids based biosensor chips integrated with electrical impedance sensor which can be sound applied on drug discovery and screening. Furthermore, it can be a promising therapy model with higher predictive value and rapid drug choice for personalized medicine as well as studying different combination of drugs' efficacy aiming at a specific disease. Besides, a multi-organs-on-a-chip platform which can be used on the research of drug effects was developed, especially focus on the side effect to other relevant organs. Overall, our works hopefully contribute to the field of drug development and precision medicine in clinical.

Acknowledgements This work was supported by National Natural Science Fund of China (No. 61320106002, 31627801, 31661143030) and National 973 project (No. 2015CB352101).

References

L.R. Arias, C.A. Perry, L. Yang, Real-time electrical impedance detection of cellular activities of oral cancer cells. Biosens. Bioelectron. **25**(10), 2225–2231 (2010)

S.S. Árnadóttir, M. Jeppesen, P. Lamy, J.B. Bramsen, I. Nordentoft, M. Knudsen, S. Vang, M.R. Madsen, O. Thastrup, J. Thastrup, Characterization of genetic intratumor heterogeneity in colorectal cancer and matching patient-derived spheroid cultures. Mol. Oncol. **12**, 132 (2018)

F. Asphahani, M. Zhang, Cellular impedance biosensors for drug screening and toxin detection. Analyst **132**(9), 835–841 (2007)

J. Bierwolf, M. Lutgehetmann, K. Feng, J. Erbes, S. Deichmann, E. Toronyi, C. Stieglitz, B. Nashan, P.X. Ma, J.M. Pollok, Primary rat hepatocyte culture on 3D nanofibrous polymer scaffolds for toxicology and pharmaceutical research. Biotechnol. Bioeng. **108**(1), 141–150 (2011)

S.C. Bürgel, L. Diener, O. Frey, J.Y. Kim, A. Hierlemann, Automated, multiplexed electrical impedance spectroscopy platform for continuous monitoring of microtissue spheroids. Anal. Chem. **88**(22), 10876–10883 (2016)

E. Fennema, N. Rivron, J. Rouwkema, C. van Blitterswijk, J. de Boer, Spheroid culture as a tool for creating 3D complex tissues. Trends Biotechnol. **31**(2), 108–115 (2013)

B. Gao, M. Peyton, C. Huang, H. Park, L. Girard, N. Sorrelle, A. Dayoub, R. Brekken, A. Gazdar, J. Minna, 3D spheroid/Organoid models of lung Cancer to study lung Cancer pathogenesis and testing of new therapeutics. J. Thorac. Oncol. **12**((8), S1544 (2017)

I. Giaever, C.R. Keese, Use of electric fields to monitor the dynamical aspect of cell behavior in tissue culture. IEEE Trans. Biomed. Eng. (2), 242–247 (1986)

M. Hay, D.W. Thomas, J.L. Craighead, C. Economides, J. Rosenthal, Clinical development success rates for investigational drugs. Nat. Biotechnol. **32**(1), 40 (2014)

L. Hu, L. Zou, Z. Qin, J. Fang, L. Huang, P. Wang, A novel label-free bioengineered cell-based biosensor for salicin detection. Sensors Actuators B Chem. **238**, 1151–1158 (2017)

G. Huang, J. Pan, Z. Ye, B. Fang, W. Cheng, Z. Cao, Overexpression of miR-216b sensitizes NSCLC cells to cisplatin-induced apoptosis by targeting c-Jun. Oncotarget **8**(61), 104206 (2017)

R.W. Jenkins, A.R. Aref, P.H. Lizotte, E. Ivanova, S. Stinson, C.W. Zhou, M. Bowden, J. Deng, H. Liu, D. Miao, Ex vivo profiling of PD-1 blockade using organotypic tumor spheroids. Cancer Discov. **8**(2), 196–215 (2018)

C.R. Keese, K. Bhawe, J. Wegener, I. Giaever, Real-time impedance assay to follow the invasive activities of metastatic cells in culture. Biotechniques **33**(4), 842–851 (2002)

K.F. Lei, T.K. Liu, N.M. Tsang, Towards a high throughput impedimetric screening of chemosensitivity of cancer cells suspended in hydrogel and cultured in a paper substrate. Biosens. Bioelectron. **100**, 355–360 (2018)

J. Li, R. Tao, W. Wu, H. Cao, J. Xin, J. Li, J. Guo, L. Jiang, C. Gao, A.A. Demetriou, 3D PLGA scaffolds improve differentiation and function of bone marrow Mesenchymal stem cell–derived hepatocytes. Stem Cells Dev. **19**(9), 1427–1436 (2010)

Y. Li, T. Zhou, C. Ma, W. Song, J. Zhang, Z. Yu, Ginsenoside metabolite compound K enhances the efficacy of cisplatin in lung cancer cells. J. Thorac. Dis. **7**(3), 400 (2015)

R.Z. Lin, H.Y. Chang, Recent advances in three-dimensional multicellular spheroid culture for biomedical research. Biotechnol. J. **3**(9–10), 1172–1184 (2008)

K. Luongo, A. Holton, A. Kaushik, P. Spence, B. Ng, R. Deschenes, S. Sundaram, S. Bhansali, Microfluidic device for trapping and monitoring three dimensional multicell spheroids using electrical impedance spectroscopy. Biomicrofluidics **7**(3), 034108 (2013)

W. Metzger, D. Sossong, A. Bächle, N. Pütz, G. Wennemuth, T. Pohlemann, M. Oberringer, The liquid overlay technique is the key to formation of co-culture spheroids consisting of primary osteoblasts, fibroblasts and endothelial cells. Cytotherapy **13**(8), 1000–1012 (2011)

K.H. Nam, A.S. Smith, S. Lone, S. Kwon, D.H. Kim, Biomimetic 3D tissue models for advanced high-throughput drug screening. J Lab Autom **20**(3), 201–215 (2015)

F. Salimi, K.A. Dilmaghani, E. Alizadeh, A. Akbarzadeh and S. Davaran, Enhancing cisplatin delivery to hepatocellular carcinoma HepG2 cells using dual sensitive smart nanocomposite. Artificial cells, nanomedicine, and biotechnology:, 1–10 (2017)

D.H. Shin, Y.J. Choi, J.W. Park, SIRT1 and AMPK mediate hypoxia-induced resistance of non–small cell lung cancers to cisplatin and doxorubicin. Cancer Res. **74**(1), 298–308 (2014)

S. Surget, M.P. Khoury, J.C. Bourdon, Uncovering the role of p53 splice variants in human malignancy: A clinical perspective. Onco Targets Ther **7**, 57 (2014)

M.W. Tibbitt, K.S. Anseth, Hydrogels as extracellular matrix mimics for 3D cell culture. Biotechnol. Bioeng. **103**(4), 655–663 (2009)

Y.C. Tung, A.Y. Hsiao, S.G. Allen, Y.S. Torisawa, M. Ho, S. Takayama, High-throughput 3D spheroid culture and drug testing using a 384 hanging drop array. Analyst **136**(3), 473–478 (2011)

C. Veelken, G.J. Bakker, D. Drell, P. Friedl, Single cell-based automated quantification of therapy responses of invasive cancer spheroids in organotypic 3D culture. Methods **128**, 139–149 (2017)

K. von der Mark, V. Gauss, H. von der Mark, P. Müller, Relationship between cell shape and type of collagen synthesised as chondrocytes lose their cartilage phenotype in culture. Nature **267**(5611), 531 (1977)

X.J. Wang, Y. Li, L. Luo, H. Wang, Z. Chi, A. Xin, X. Li, J. Wu, X. Tang, Oxaliplatin activates the Keap1/Nrf2 antioxidant system conferring protection against the cytotoxicity of anticancer drugs. Free Radic. Biol. Med. **70**, 68–77 (2014)

L. Zou, C. Wu, Q. Wang, J. Zhou, K. Su, H. Li, N. Hu, P. Wang, An improved sensitive assay for the detection of PSP toxins with neuroblastoma cell-based impedance biosensor. Biosens. Bioelectron. **67**, 458–464 (2015)